PROCEEDINGS OF SPIE

SPIEDigitalLibrary.org/conference-proceedings-of-spie

Direct measurement of a nonequilibrium system entropy using a feedback trap

Momčilo Gavrilov, John Bechhoefer

SPIE.

Invited Paper

Direct measurement of a nonequilibrium system entropy using a feedback trap

Momčilo Gavrilov[a] and John Bechhoefer

Department of Physics, Simon Fraser University, Burnaby, BC, V5A 1S6 Canada

ABSTRACT

Feedback traps are tools for trapping single charged objects in solution. They periodically measure an object's position and apply a feedback force to counteract Brownian motion. The feedback force can be calculated as a gradient of a potential function, effectively creating a "virtual potential." Its flexibility regarding the choice of form of the potential gives an opportunity to explore various fundamental questions in stochastic thermodynamics. Here, we review the theory behind feedback traps and apply it to measuring the average work required to erase a fraction of a bit of information. The results agree with predictions based on the nonequilibrium system entropy. With this example, we also show how a feedback trap can easily implement the complex erasure protocols required to reach ultimate thermodynamic limits.

Keywords: feedback trap, nonequilibrium entropy,information entropy, Maxwell's demon, Szilard engine, virtual potential

1. INTRODUCTION

Thermodynamics explores laws of nature that govern processes of work, heat, matter, and information exchange among systems, subsystems, and their environments. It applies to all systems in nature and sets constraints on permissible physical processes, as formulated in four basic laws.[1] As a consequence of those fundamental laws, the total entropy in any process never decreases, which puts fundamental limits on the energy efficiency of heat engines, refrigerators, and computations. Although the probabilistic nature underlying many processes in thermodynamics has been suggested since the middle of the 19th c.,[1] experiments on such systems were traditionally based on macroscopic manipulations of many constituents and observations of their mean behavior, or, at best, on low-order moments of fluctuations.

Only in the past few decades have experimental tools become widely available for microscopic thermodynamic manipulations of small, fluctuating systems with energy resolutions below kT.[2] These developments have been accompanied by significant advances in theory, culminating in the development of a new field, *stochastic thermodynamics*,[3,4] for treating thermodynamics in systems that are small enough that fluctuations play an essential role. As a result, we now can directly control the individual constituents of a system and use that control to test experimentally the foundations of thermodynamics and statistical physics in a way that previously could be done only via highly idealized "thought experiments."

One hundred and fifty years ago, Maxwell suggested one such thought experiment, where an intelligent creature—*a demon*—has the ability to acquire information about each individual molecule in a gas and use it for doing work.[5,6] Later, the probabilistic nature of the thermodynamics became detectable,[7,8] and measurements where the outcome depends on how much information about the system is acquired became possible.[9] This led to the design of the first information engines,[9,10] which use information reservoirs to extract work or cool the system or alternatively use energy to erase or modify information.[11,12]

These tests of thermodynamic systems at the molecular scale have been possible only because of the development of new experimental techniques. In this paper, we present a relatively recent technique for such studies, the *feedback trap* and compare it to more traditional techniques such as optical tweezers. The feedback trap is a tool

Further author information: Send correspondence to MG, momcilog@sfu.ca, or JB, johnb@sfu.ca.
[a] Present address: Department of Biophysics and Biophysical Chemistry, Johns Hopkins University, 725 N. Wolfe Street, Baltimore, MD 21205-2185, USA

Optical Trapping and Optical Micromanipulation XIV, edited by Kishan Dholakia, Gabriel C. Spalding,
Proc. of SPIE Vol. 10347, 103470U · © 2017 SPIE · CCC code: 0277-786X/17/$18 · doi: 10.1117/12.2277602

suitable for exploring a broad spectrum of problems in this field, because of its unique flexibility in the choice of a potential and ways to manipulate it. In this paper, we present an experiment where less than one bit of information is erased, and we measure the minimal work to carry out this operation. Our memory is represented by a silica bead trapped in a "virtual" time-dependent double-well potential, created by a feedback loop. The major challenge is to design a *thermodynamically reversible* protocol capable of reaching the minimal work.[13] As we show in Sec. 5.2, such a protocol requires complex control involving barrier height, tilt, and local coordinate stretching to produce asymmetry between macrostates and operate close to equilibrium. These manipulations are easy to achieve using feedback traps, where the form of a virtual potential is defined in software by applying the force at each measured position that would be applied by a physical potential. In this paper, we also compare the feedback trap with other tools and techniques for micromanipulation and discuss their application to stochastic thermodynamics.

2. MEASUREMENTS IN STOCHASTIC THERMODYNAMICS

Several important advances in science and technology have made possible measurements on small systems that, before, could exist only in thought experiments. They allow one to test fundamental limits for processes in stochastic thermodynamics. These advances can be roughly classified in two groups: technical, which includes the ability to manipulate the small objects; and conceptual, which is the ability to estimate thermodynamical quantities for a single object in a medium.

2.1 Experimental techniques in stochastic thermodynamics

Many tools for micromanipulation, predominately used in biology and biophysics have also proven useful for measurements in stochastic thermodynamics. Because the amount of work needed to manipulate the system is comparable to the thermal fluctuations, the intrinsic dissipation of the tool should not perturb the system significantly. In our studies, we use one of these new tools, a feedback trap. To motivate its choice, we first introduce the feedback trap and some alternative tools,[2] so that we can better understand the special features of our technique. Later, in Sec. 4, we provide a more detailed description of feedback traps.

2.2 Feedback or ABEL trap

Feedback or Anti-Brownian ELectrokinetic (ABEL) traps[14] are tools for trapping and manipulating single charged objects, such as molecules in solution. They have been developed as an alternative to optical tweezers and other single-molecule techniques. They use feedback to counteract the Brownian motion of a molecule of interest. Since they also can counteract other types of motion caused by mechanical or electrical drifts and can also use forces that are not electrokinetic, we refer to them more generically as *feedback traps*. In its original implementation by Cohen and Moerner,[14] the trap first acquires information about a molecule's position and then applies an electric feedback force to move the molecule. Since electric forces are stronger than optical forces at small scales,[15] feedback traps are the best way to trap single molecules without "touching" them (e.g., by putting them in a small box or attaching them to a tether).

Feedback traps can do more than trap molecules: They can also subject a target object to forces that are calculated to be the gradient of a desired potential function $U(x,t)$.[15] If the feedback loop is fast enough, it creates a *virtual potential* whose dynamics will be very close to those of a particle in an actual potential $U(x,t)$. But because the dynamics are entirely a result of the feedback loop—absent the feedback, there is only an object diffusing in a fluid—we are free to specify and then manipulate in time an arbitrary potential $U(x,t)$. In our work presented here, we have improved the stability and accuracy of measurements of feedback traps to the point that we can use them for sensitive experiments in stochastic thermodynamics.[16]

2.2.1 Optical tweezers

In 1986, Arthur Ashkin showed that a tightly focused beam of light can attract and confine a micron-sized particle in a solution.[17] The typical trapping force induced by a tightly focused laser beam on a micron-size bead is on the order of 1 pN, which makes optical traps suitable for probing energies of order kT, the average energy per degree of freedom ($kT \approx 4$ pN $\times$ nm at $T \approx 300$ K). The optical trap can be used for two distinct

types of experiment. In the first, the potential induced by the optical trap is the subject of a direct study, while in the second type, optical forces are used to probe some other stochastic system, such as a single molecule.

The optical trap, in principle, allows one to impose potentials of several different forms. For example, two nearby traps can together create a double-well potential. Alternatively, varying the intensity of the laser light allows one to control the stiffness of the harmonic trap near the potential minimum. Several calibration methods were developed to establish the connection between the stiffness and the laser intensity.[18,19] The optical trap can be combined with a piezoelectric motor to move the trapping bead relative to the surrounding fluid. Wang et al. demonstrated the importance of fluctuations in small systems and showed the long-anticipated probabilistic nature of the second law of thermodynamics.[7] In combination with the acousto-optic laser deflector (AOD), the optical tweezers were used to test the Landauer principle.[11]

Single molecules are another example of stochastic system that can be manipulated by optical tweezers and further used in stochastic and nonequilibrium thermodynamics. For example, a single RNA hairpin was manipulated using optical tweezers to test the Jarzynski work-fluctuation theorem[8] and, later, the Crooks theorem.[20]

2.2.2 Electric and magnetic forces

Small objects in solutions are usually electrically charged and can be manipulated by electric fields in a process called electrophoresis. Even if the object is not charged, one can still move it in a fluid using an electroosmotic flow in the presence of the electric field. Although the electric field can have local minimum for passive trapping such as in a *corral trap*,[21] it is often implemented together with feedback or used to modify the optical force. In one of the first information engines, Toyabe et al. used position information to make a particle climb up a spiral-staircase-like potential created by an electric field.[9] In another study that combines optical and electric forces, Roldán et al. explored how sudden changes in ergodicity affect the thermodynamics of a colloidal bead and explored memory erasure as the restoration of a broken symmetry.[22] Electric forces can, in some cases, be an additional source of fluctuations. This opened a possibility for coupling a system to several different thermal baths and operating a first Brownian Carnot engine.[23,24] This approach is different from heating a surrounding fluid directly by a laser.[25]

2.2.3 Thermally driven, hydrodynamic, and acoustic traps

Braun et al. developed a new single-molecule-trapping concept that uses a temperature gradient to counteract Brownian motion.[26] This method locally heats the fluid around a trapped particle and can be used with or without a feedback. It spatially and temporally varies the temperature at a plasmonic nanostructure and induces thermodiffusive drifts.

Hydrodynamic traps can manipulate small objects by creating flows of a surrounding fluid. The moving fluid can displace objects with sufficient drag and confine them in a small region.[27,28] They can also be combined with a feedback to stabilize a particle at the desired point.[29–32]

2.3 Single-particle stochastic thermodynamics

Sekimoto introduced an important conceptual advance for extending thermodynamical ideas to small systems. He proposed a method for determining the stochastic energetics of a particle solely from its Langevin dynamics.[3,33] In practice, the thermodynamical quantities work and heat can be estimated from a particle's trajectory $x(t)$ and the shape of the potential $U[x, \lambda(t)]$, that can be controlled using a time dependent protocol or parameter $\lambda(t)$. In particular, determining the stochastic energetics does not rely on measuring directly the minute amounts of heat ($1\ kT \approx\ 10^{-21}$ J), which is a typical energy scale for many stochastic processes. This method was tested, for example, by studying a colloidal particle in an aqueous medium.[34] Extensions have led to a new field, stochastic thermodynamics, which is the natural formalism for describing small systems.[4,35] By focusing solely on the trajectory and the potential, one can isolate and measure the quantities of direct interest. This method removes the contributions of work and dissipation from ancillary devices—computer, camera, illumination, etc.—that are irrelevant to calculating the work done by the potential on the particle and the heat dissipated into the surrounding bath.

2.3.1 Stochastic heat and work

Many of the experimental techniques described in Sec. 2.1 manipulate a single particle in a potential $U[x, \lambda(t)]$ via a *control parameter* $\lambda(t)$ to find the stochastic work and heat exchanged with a bath. The change in total energy of a particle confined in a potential is

$$dE = dU = (\partial_x U)dx + (\partial_\lambda U)d\lambda\,. \tag{1}$$

For a particle in equilibrium in a constant potential $U(x, \lambda = \text{const})$, no work is done, and $dW = 0$. The energy of the particle depends only on where the particle is in the potential $dE = (\partial_x U)dx$. From the first law, $dE = dW - dQ$, and the energy in Eq. 1, the heat released to the bath is

$$dQ = dE|_{\lambda=\text{const.}} = (\partial_x U)dx\,. \tag{2}$$

For an equilibrium system at constant temperature T, a particle in a static potential continuously exchanges heat with the bath, but there is no net heat exchange on average.

Applying work to the particle requires a time-dependent potential $U[x, \lambda(t)]$. The work to change the potential while the particle remains at the position x is

$$dW = (\partial_\lambda U)d\lambda\,. \tag{3}$$

Finally, to find the total work and heat released to the bath during a protocol of duration τ, we integrate Eq. 2 and Eq. 3 over time. The total work is

$$W = \int_0^\tau \partial_\lambda U(x, \lambda)|_{x(t)}\, \dot{\lambda} dt\,, \tag{4}$$

and the heat exchanged is

$$Q = \int_0^\tau \partial_x U(x, \lambda)|_{x(t)}\, \dot{x}(t)\, dt = -\int_0^\tau F\dot{x} dt\,. \tag{5}$$

When $\lambda(t) = t$, the work estimate in Eq. 4 simplifies to

$$W = \int_0^\tau \partial_t U(x, t)|_{x(t)}\, dt\,. \tag{6}$$

Although one can use Eqs. 5 and 6 to estimate heat and work directly, the result will be more accurate if one estimates only the average work and then infers the heat using the first law of thermodynamics.[36] Also, since the work estimate is insensitive to the discretization scheme in use, which is not the case with the heat, we focus solely on work estimates.

2.4 Fluctuation theorems

Traditional thermodynamics describes irreversible processes with inequalities. For example, the second law can be expressed as the Clausius inequality $W \geq \Delta F$, which puts a lower constraint on the average work in any process. In 1997, Jarzynski showed that this relationship can be the consequence of a more general equality, commonly referred to as the work-fluctuation theorem or Jarzynski equality.[37] This theorem can be applied to any system arbitrarily far from equilibrium. Here, we briefly introduce the Jarzynski equality and Crooks theorem, which is a related equality describing non-equilibrium transformations. Both expressions require the temperature of the bath to be well defined, which is the case for our isothermal experiments.

2.4.1 Jarzynski equality

In any nonequilibrium process or transformation starting in an equilibrium state, the Jarzynski fluctuation theorem quantifies the work to change the free energy of the initial equilibrium state by the amount* ΔF as

$$\left\langle e^{-W/kT} \right\rangle = e^{-\Delta F/kT} , \tag{7}$$

where the left-hand side of Eq. 7 is an exponential average over the work distribution $p(W)$:

$$\left\langle e^{-W/kT} \right\rangle = \int_{-\infty}^{+\infty} p(W) e^{-W/kT} dW . \tag{8}$$

The Jarzynski equality allows one to estimate the free-energy difference, an equilibrium property, from nonequilibrium measurements. For example, if a system is driven via a controllable potential $U[x, \lambda(t)]$ from the initial equilibrium state $[\lambda_0 = \lambda(0)]$ to the final state $[\lambda_\tau = \lambda(\tau)]$, the free-energy difference between two states can be estimated from Eq. 7 by calculating the exponential average of the measured work values. It is not required for the system to be in equilibrium at the end of the protocol, because any further relaxation to equilibrium, without change in λ, does not contribute to the work.

For certain classes of work distributions, Eq. 7 can be simplified. If the work distribution is Gaussian, then

$$\sigma_W^2 = \frac{2}{kT} \left(\langle W \rangle - \Delta F \right) , \tag{9}$$

where σ_W^2 is the dimensionless variance in work scaled by kT. Equation 9 gives a transparent expression for estimating ΔF from the mean and variance. The Jarzynski equality has been tested in many experiments.[8,38–41] It is also a common method to estimate free energy landscapes for proteins.[35,42,43]

2.4.2 Crooks and detailed fluctuation theorem

The Crooks fluctuation theorem states that observing a trajectory of a time-reversed process is exponentially less likely than observing the same trajectory in a forward process. The Crooks theorem has very broad application, as it holds for trajectories in any phase space. For the purpose of work measurements, the Crooks theorem is useful for linking work done in forward and time-reversed processes.

The detailed fluctuation theorem links the two processes in a quantitative way. The probability $p(\Lambda_x)$ of system taking a trajectory Λ_x in a forward process is exponentially more likely than the probability $\tilde{p}(\widetilde{\Lambda_x})$ of retracing backwards the same trajectory when the protocol is reversed:

$$\frac{p(\Lambda_x)}{\tilde{p}(\widetilde{\Lambda_x})} = e^{\{W[x(t)] - \Delta F\}/kT} , \tag{10}$$

where $\widetilde{\Lambda_x}$ denotes the time-reversed trajectory..

In Eqs. 7 and 10, ΔF is the change in free energy between the final and initial states. The work along trajectory Λ_x in the forward direction is $W_F(\Lambda_x)$, while the work along the same trajectory is $W_R(\widetilde{\Lambda_x})$ when time reversed.† Below, we simplify the notation and use $W \equiv W_F(\Lambda_x)$

A work value W can be calculated from several different trajectories, but only one trajectory Λ_x corresponds to only one work value in Eq. 4. By averaging over all trajectories corresponding to a single work value W, the probabilities of measuring that work value W in a forward $p_F(W)$ and $-W$ in the corresponding reverse $p_R(-W)$ process can be written as the *Crooks relation*

$$\frac{p_F(W)}{p_R(-W)} = e^{(W - \Delta F)/kT} , \tag{11}$$

* The definition of free energy difference here is between the final and the initial state $\Delta F = F_{\text{final}} - F_{\text{initial}}$.

†Time reversal is just a mathematical abstraction. No experimentalist can reverse time and measure work while "undoing" the experiment. She or he can only run the reversed protocol forward in time and measure work, while assuming this to be equivalent to time reversal.

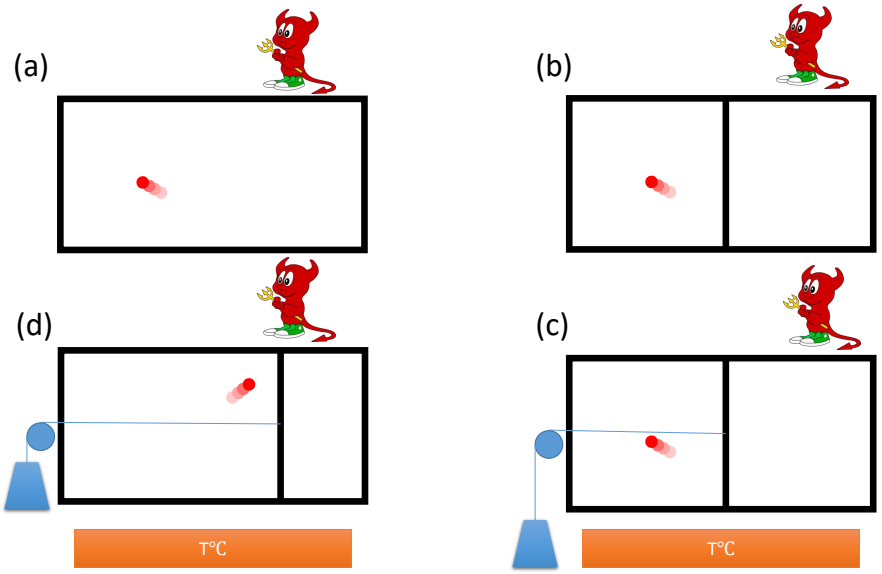

Figure 1. Szilárd engine. (a) Single gas molecule in a box. (b) The demon splits the volume in two and measures the location of a single molecule. (c) Based on the molecule's position, the demon attaches "the gear" for extracting mechanical work and couples the system to a thermal bath. (d) In an isothermal process, the heat is transferred from the bath and converted to the mechanical work. Demon illustration from Ref. 47.

3. INFORMATION AND THERMODYNAMICS

Information, thermodynamics, and the probabilistic nature of the second law were implicitly linked in two historical thought experiments, Maxwell's demon (1871) and the Szilárd engine (1929). Later, in the 1940s, the scientific community tried to determine the minimum power for a computation. When the first electronic computers became available, John von Neumann proposed that any computation necessarily releases heat and requires work for operation.[44] Surprisingly, in 1961, Rolf Landauer, recognizing the physical nature of information, showed that only logically irreversible operations require work;[45] however, if the operation is logically reversible, in principle it could be done without work.

3.1 Maxwell's demon and Szilárd engine

The probabilistic nature of the second law of thermodynamics is well illustrated by Maxwell's demon, a thought experiment introduced to the public by James Clerk Maxwell in his book *Theory of Heat* in 1871.[5] The demon is an intelligent agent or creature capable of measuring the speed of individual molecules in a gas. It further uses that information to create a temperature gradient and push the system out of equilibrium, to extract work.

Maxwell's demon is the first discussion of the role that feedback plays in thermodynamics, showing how the demon's measurement based on the acquired information can alter the thermodynamics of a system. Maxwell did not explicitly discuss information collected by the demon; information was introduced to thermodynamics later in a stylized version of a demon, the Szilárd engine.

Leó Szilárd linked information to thermodynamics for the first time in 1929, when he proposed a thought experiment with a single molecule gas.[46] Instead of continuous information about a speed, his demon collects binary information about a molecule's position, whether it is in the left or the right half of the box. The demon, illustrated in Fig. 1, splits the box into two equal volumes with a movable piston. Depending on the information about the position, the demon now lets the single-molecule gas isothermally expand to the right (or left) and do work.

In this original setup, the demon operates with maximal efficiency and collects the most meaningful data.[48] Only under such circumstances, the maximal amount of work per cycle that the Szilárd engine can do is $kT \ln 2$. The amount of meaningful information that the demon acquires about the system, per cycle, is 1 bit $= \ln 2$ nat.

This demon can, in principle, run indefinitely and extract work from the bath for ever. The demon has puzzled many scientists over the years. Leó Szilárd,[46] Léon Brillouin,[49] and others[6] proposed that the measurement step is inherently dissipative. Indeed, this is the case for some special systems,[49] where the demon spends more energy on the measuring process than it can extract from the system; however, Charles Bennett showed that measurements can, in principle, be done without work.[50] Bennett and, independently, Oliver Penrose[51] concluded that if measurements and calculations do not require work, the only other possibility consistent with the second law is that the erasure step, required to return the demon's memory to its original state, is dissipative. Thus, Landauer's principle resolves the paradox created by Maxwell's demon. In other words, Maxwell's demon can extract work from the bath as long as it can acquire information about the gas.[6]

In the past, there have been other proposals and objections about the design of this type of thought experiment: for example, is the pressure a single molecule exerts on a piston smooth enough to calculate work from the ideal-gas equation? From a quantum-mechanical point of view, measuring a molecule's location alters its position, too. It was later clarified that this was not relevant. Detailed discussion about such ideas can be found in Ref. 6.

4. FEEDBACK TRAPS

In 2005, Cohen and Moerner developed a new tool for trapping and manipulating small objects, such as single molecules, in solution.[14] This new tool, which we call a *feedback trap*, is an alternative to optical tweezers and other single-molecule techniques. It uses feedback to counteract the Brownian motion of a molecule of interest. The trap first acquires information about a molecule's position and then applies an electric feedback force to move the molecule. Since electric forces are stronger than optical forces at small scales, feedback traps are the best way to trap single molecules without "touching" them (e.g., by putting them in a small box or attaching them to a tether).

Feedback traps can do more than trap molecules: They can also subject a target object to forces that are calculated to be the gradient of a desired potential function $U(x)$. If the feedback loop is fast enough, it creates a *virtual potential* whose dynamics will be very close to those of a particle in an actual potential $U(x)$. But because the dynamics are entirely a result of the feedback loop—absent the feedback, there is only an object diffusing in a fluid—we are free to specify and then manipulate in time an arbitrary potential $U(x,t)$.

4.1 Operation of a feedback trap

Feedback traps have been applied to the study of single molecules[15,52–58] and to explore fundamental questions in the non-equilibrium statistical mechanics of small systems.[12–15,41,59–63] Depending on the intended application, feedback traps differ in their design. For the study of single molecules, the feedback trap has to be able to trap a fast-diffusing, dim molecule; as a result, it is usually implemented with a fast-scanning laser beam.[53] Each time the laser beam hits a molecule, a photon can be emitted and detected by a photo diode. The position of a molecule can be inferred from the laser position at the time of a photon detection and later used to counteract the displacement due to the Brownian motion.

For the application in stochastic thermodynamics, which is the main focus of this article, the feedback trap has to be able to operate over days-long experiments and collects large amount of statistical data. Our camera-based feedback trap is implemented around a home-built inverted microscope.[16,59,61] We trap silica beads of nominal diameter 1.5 μm immersed in water. The beads are heavy enough to sink to the bottom of the sample cell and stay in focus in the microscope but light enough to diffuse laterally. Thus, gravity balances electrostatic repulsion from the bottom and confines particles vertically. Two sets of electrodes control the electric field in the x and y directions, applying the desired force to the particle.

Figure 2 shows one cycle of a feedback trap in operation.[16,59] The camera first images a particle using a dark-field microscope. From the image, the particle position $\bar{x}_n$ is estimated using a centroid algorithm,[64] and the feedback force is calculated from the chosen potential $f_x = -\partial_x U(x,t)$, evaluated at the observed position $\bar{x}_n$. Finally, the feedback trap applies a voltage V_n that is calibrated to correspond to the desired force f_n, which moves the particle. The voltage is kept constant for $\Delta t = 5$ ms and then updated with a delay $t_d = 5$ ms relative to the exposure midpoint.

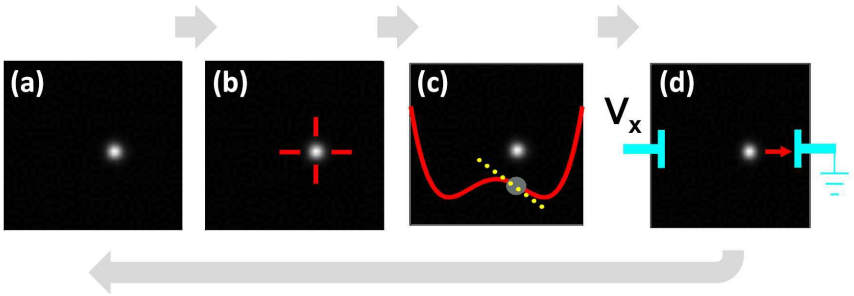

Figure 2. Schematic of feedback-trap operation. (a) Acquisition of an image of a fluorescent particle. (b) Determination of particle position from that image using a centroid algorithm. (c) Evaluation of feedback force $f_x = -\partial_x U(x,t)$ at the observed position $\bar{x}$. (d) Application of electric force, with voltage set by electrodes (light blue), held constant during the update time $\Delta t = 5$ ms. The long gray arrow indicates repetition of the cycle. Figure reproduced from Ref. 41.

In the original version of the feedback trap[14] and in our first version,[16,59] as well, the imaging was based on fluorescence illumination, as is appropriate for fluorescent particles and for labeling individual molecules in solution. In such low-light conditions, camera-based imaging systems need to integrate all the time to capture as much information from a fluorescent particle as possible, leading to a camera-exposure time $t_c = \Delta t$. Even with such a long exposure, the overall light levels are low, implying significant observation noise due to photon shot noise and the diffraction limit of the microscope. In the much brighter scattering-based illumination described above, the camera time can be short ($t_c/\Delta t \leq 0.1$) and the measurement noise can be small.[61] The simplified theoretical description developed below takes advantage of this improved illumination scheme.

4.2 Trap dynamics

The low-frequency stochastic dynamics of a Brownian particle are well described by a Langevin equation in the overdamped limit. For a one-dimensional trajectory $x(t)$, the Langevin equation is

$$\gamma\,\dot{x} = f(x,t) + \xi^{(f)}(t)\,, \tag{12}$$

where γ is the drag coefficient, $\xi^{(f)}(t)$ is the fluctuating thermal force acting on the particle, and $f(x,t)$ is the external force. Here, the force $f(x,t) = -\partial_x U(x,t)$ is chosen to be the gradient of a time-dependent potential $U(x,t)$. In Eq. 12, we have neglected the mass term, $m\ddot{x}$, as the inertial time scale, m/γ, is of order microseconds, whereas experimental time scales are of order milliseconds.

Although Eq. 12 is one dimensional, the particle moves in three dimensions. We have already discussed how gravity and electrostatic forces naturally confine the motion in z. For the lateral y-direction, we confine the particle by adding a static harmonic component, so that $U(x,y,t) = U(x,t) + \frac{1}{2}\kappa y^2$. The y motion then plays no role in work and heat estimates and is ignored in the rest of the analysis, which focuses on the one-dimensional motion along x.

To discretize Eq. 12, we integrate it over the time interval $[t_n, t_{n+1})$, where $t_n \equiv n\Delta t$ and Δt is the feedback cycle time. The force is kept constant in that time interval: $f(x,t) \equiv f_{n-1}$, for $t \in [t_n, t_{n+1})$. The discretized position of the particle (x_n) at the beginning of that interval (t_n) is

$$x_{n+1} = x_n + \tfrac{\Delta t}{\gamma} f_{n-1} + \xi_n\,, \qquad \xi_n = \frac{1}{\gamma}\int_{t_n}^{t_{n+1}} dt\,\xi^{(f)}(t)\,. \tag{13}$$

In Eq. 13, ξ_n represents the displacement due to thermal forces that are integrated over the cycle time Δt of a single time step. The displacements are described by i.i.d. random Gaussian variables with mean 0, and variances $\langle \xi_n^2 \rangle = 2D\,\Delta t$, with D the lateral diffusion coefficient of the particle. As discussed above, in general, we would supplement Eq. 13 with a second equation for the observed position, which incorporates effects due to exposure averaging, measurement noise, and the rather subtle noise correlations that follow.[12] Fortunately, these are all small effects in the current setup and will be ignored here.

To simplify the equation of motion, let us introduce coordinates where lengths are scaled by $\ell = \sqrt{D\Delta t}$ and energies by kT. We also use the Einstein relation $D = kT/\gamma$. More formally, we define (omitting the time subscript for simplicity),

$$x' = \frac{x}{\ell}\,, \qquad \xi' = \frac{\xi}{\ell}\,, \qquad U' = \frac{U}{kT}\,, \qquad f' = \frac{\ell f}{kT}\,, \qquad t' = \frac{t}{\Delta t}\,. \tag{14}$$

In terms of these scalings, Eq. 13 becomes

$$x'_{n+1} = x'_n + f'_{n-1} + \sqrt{2}\,\xi'_n\,, \qquad f'_{n-1} = -\left.\frac{\partial U'(x',t')}{\partial x'}\right|_{x'=x'_{n-1},\,t'=n-1}\,. \tag{15}$$

Note the $n-1$ subscript for the force term, which reflects the unit delay of the feedback system. In our experimental design, we take care to make sure that the updated force is applied precisely at a time Δt after the midpoint of the exposure, as this is necessary in the simplified equations we give here. We note that the experiment is particularly sensitive to timing variations and that using "real time" programming techniques and hardware is important. Finally, in Eq. 15, the scaled noise terms ξ'_n are independent Gaussian random variables with $\langle \xi'_n \rangle = 0$ and $\langle {\xi'_n}^2 \rangle = 1$.

An important special case is a harmonic potential, $U = \frac{1}{2}\kappa x^2$, or $U' = \frac{1}{2}\alpha x'^2$, where $\alpha = \kappa\ell^2/kT = \kappa\Delta t/\gamma = \Delta t/t_r$. In the last version, t_r is the relaxation time of an overdamped particle in a harmonic potential. More generally, we can replace κ by $\partial_{xx}U(x,t)$, evaluated at the bottom of a local potential well. For a harmonic potential, the scaled equation of motion is

$$x'_{n+1} = x'_n - \alpha\, x'_{n-1} + \sqrt{2}\,\xi'_n\,. \tag{16}$$

Earlier study explores in details the dynamics and thermodynamics of a particle in a virtual harmonic potential and takes into account the delay, exposure time, and the observational noise.[12] If the relaxation time of the potential is much greater than the update time of the feedback trap $t_r \gg \Delta t$ or $\alpha = \Delta t/t_r \to 0$, the dynamics approaches the dynamics of a particle in a physical potential. In our experiment, the feedback gain never exceeds $\alpha = 0.2$, which affects the work in a virtual potential. Nevertheless, for a cyclic protocol, where the potential is the same at the beginning and the end of a protocol, the correction term cancels out and the work measurement is exact.[62]

4.3 Trap calibration

The energy scale of the processes we consider are of order $kT \approx 4 \times 10^{-21}$ J, where T is the temperature of the heat bath the system is immersed in and k is Boltzmann's constant. For detecting such small energy changes in protocols that can last minutes, we need careful, high-precision calibration techniques that can convert the applied voltages into precisely known forces.[16] Here, we briefly summarize the calibration process.

Rearranging Eq. 15 for the feedback trap dynamics, we write $\Delta x'_n \equiv x'_{n+1} - x'_n = f'_{n-1} + \sqrt{2}\,\xi'_n$ for the displacement. Thus, the displacement results from a deterministic component, f', which we control, and a stochastic component, ξ', which we do not. To control the forces f'_{n-1}, we apply a voltage V_{n-1}, which generates an electric field that moves the charged particle to a new position. In other words, the controllable component of displacement f'_{n-1} is proportional to the applied voltage as $f'_{n-1} = \mu\,\Delta t\,(V_{n-1} + V_\mathrm{o})$, where μ is the mobility (response) of a charged particle (in an ionic fluid) to the applied voltage. The offset V_o arises from electrochemical reactions at the electrodes and from the amplifier in the circuit. The link between displacement $\Delta x'_n$ and applied voltage is then

$$\Delta x'_n = \mu\,\Delta t\,V_{n-1} + \mu\,\Delta t V_\mathrm{o} + \sqrt{2}\,\xi'_n\,. \tag{17}$$

In principle, we could estimate μ and V_o as the slope and intercept in a linear, least-squares fit to N measurements and could similarly infer the diffusion coefficient D from the residuals. However, our goal is to implement a continuous calibration, and we cannot afford to recompute such a fit at every time step in the experiment. Fortunately, it has long been known that linear least-squares fits have a *recursive* formulation where existing estimates of slope and intercept are updated each time a new data point arrives.[65] Here, in order to treat small

noise correlations (arising from term neglected in Eq. 13), we use a slight generalization known as *Recursive Maximum Likelihood* (RML).[16,65]

One complication is that experimental parameters slowly drift due to temperature drifts and electrochemical reactions. We thus limit the amount of the past time series measurements that enter into the calibration by using a *running average* variant of the RML algorithm that weights new versus old measurements.[16]

The RML algorithm is similar to a simplified version of the *Kalman filter*,[66] except that in RML case, the changes in parameters μ and D are traced by time-averaging.

Another complication is that the feedback trap corrects motion in two dimensions. Since the electric-field lines are not exactly aligned along the x-y axes (defined by the camera pixels), we need to implement a full two-dimensional version of the RML algorithm that accounts for coupling between axes. Apart from generalizing the mobility μ to a two-by-two matrix $\boldsymbol{\mu}$ and the offset voltage to a vector $\mathbf{V}_0$, the algorithm is identical.

5. EXAMPLE: FEEDBACK TRAP FOR MEASUREMENTS IN STOCHASTIC THERMODYNAMICS

In this final section, we apply a feedback trap to the problem of erasing less than one bit of information. Our system is a silica particle trapped in a symmetric double-well potential, which is allowed to take an asymmetric form during erasure. We test two different protocols to erase such an incomplete memory. Our first, naive protocol, does not reach the limit presented in Sec. 5.2, while adding extra steps to the protocol makes reaching such limits possible.

5.1 Virtual double-well potential

Our virtual double-well potential has x and y components that are programmable in our LabVIEW code. The potential in z is physical, where the gravitational force keeps the particle at the bottom of a trapping region. The virtual potential is static harmonic in t he y direction. In the x direction, the potential has a double-well form. One of the wells can be selectively stretched. The functional form for our potential is

$$U(x,t) = 4E_{\mathrm{b}}\left[-\tfrac{1}{2}g(t)\,\tilde{x}^2 + \tfrac{1}{4}\tilde{x}^4 - Af(t)\,\tilde{x}\right], \tag{18}$$

where the scaled coordinate $\tilde{x}(x,t)$ is selectively stretched for positive or negative x, as desired. More precisely, $\tilde{x}(x<0,t) = -\tilde{\eta}(t)\tilde{x}(x\geq 0,t)$ where $\tilde{\eta}(t)$ is a time-dependent stretching factor. Note that the stretching amplitude η scales the stretching factor $\tilde{\eta}(t)$. In all cases, $\tilde{\eta}(0) = \tilde{\eta}(\tau) = 1$, so that we start and end with a symmetric potential. In Eq. 18, E_{b} is the energy barrier height, A the tilt amplitude. The functions $g(t)$ and $f(t)$ can take values between 0 and 1 and control the barrier height and tilt. Together with stretching $\tilde{\eta}(t)$, they allow us to implement various protocols.

5.2 Partial memory erasure

Using the potential in Eq. 18, we can encode less than one bit of memory. This is achieved by placing a particle in the left well with the probability p_0. For a total number of measurements N, we place a particle to the left well $p_0 N$ times and to the right well $(1-p_0)N$ times. We can then estimate the Shannon entropy $H[p(t)]$ in bits as

$$H(p) = -p\log_2 p - (1-p)\log_2(1-p)\,, \tag{19}$$

where p is the probability to find a particle in range $x \subset (-\infty, 0]$.

Our goal is to estimate the minimal average work to erase less than one bit of memory. This work is[67]

$$\langle W\rangle_{\mathrm{min}} = kT(\ln 2)\left[H(p_\tau) - H(p_0)\right], \tag{20}$$

where p_0 and p_τ are probabilities before and after erasure. For the full erasure $p_\tau = 0$ and the average work is

$$\langle W\rangle_{\mathrm{min}} = -kT(\ln 2)H(p_0)\,, \tag{21}$$

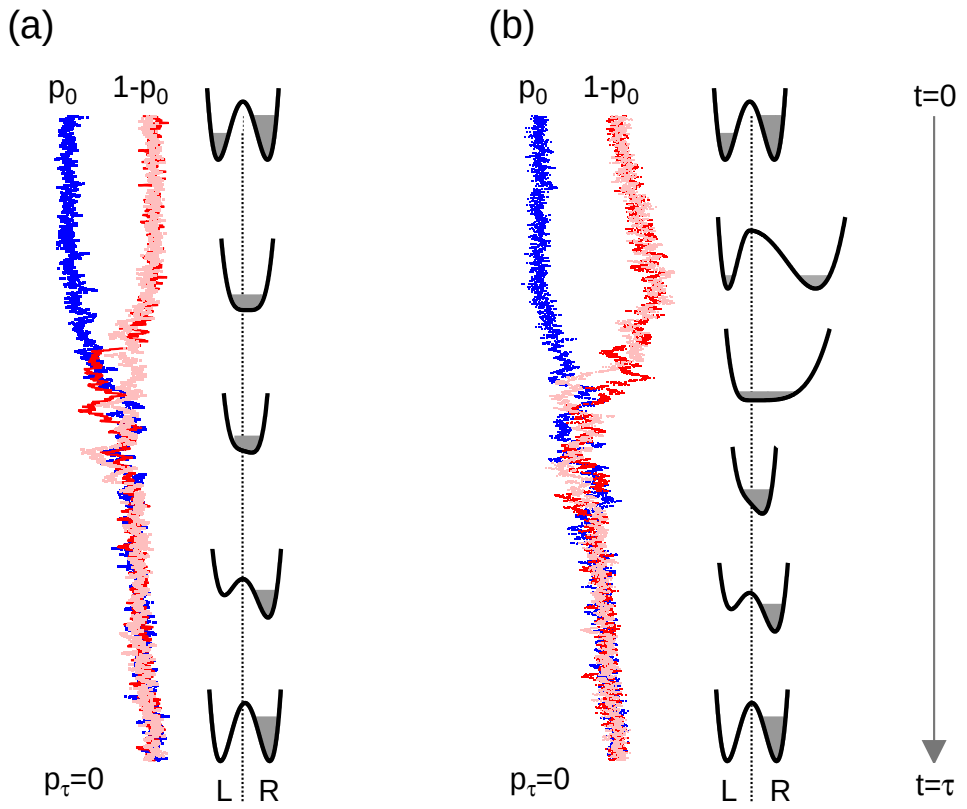

Figure 3. Comparison between work in Protocols 1 and 2. Recorded trajectories are shown next to the potential. Both protocols start with information $H(\frac{1}{3})$, indicated by one out of three trajectories starting in the left well. (a) Protocol 1 directly mixes two states to erase the memory and return the potential to its initial form while keeping particles in one well. (b) Protocol 2 brings the system to a global equilibrium by stretching the right well and then erasing memory as in Protocol 1.

Here, we explore only the case where the system starts in the left well with probability $p_0 = \frac{1}{3}$; therefore we can directly estimate the minimal work in Eq. 21, $\langle W \rangle_{\min}(\frac{1}{3})/kT = (\ln 2)\, H(\frac{1}{3}) \approx 0.64$. We further present two protocols and test whether they can reach the minimal work value (Eq. 21) in an arbitrarily slow limit. Protocol 1 allows two states to interact directly, while the Protocol 2 brings the system to a global equilibrium first and then allows for the interaction between states. We will see that only Protocol 2 can reach the limit in Eq. 21.

5.2.1 Protocol 1

Protocol 1 is depicted in Fig. 3 (a). This protocol starts from a symmetric double-well potential, encoding information $H(p_0)$, and a high energy barrier $E_b/kT = 13$. We first lower down the barrier. This is achieved by decreasing the value of the function $g(t)$ from 1 to 0. In next step, we tilt the potential. The tilt amplitude is set to $A = 0.2$, while the tilting is achieved by increasing the value of the function $f(t)$ from 0 to 1. This strong tilt assures that all trajectories end in the right-hand well with $p_\tau = 0$. Finally, we increase the barrier back to $E_b/kT = 13$ and untilt. Typical particle trajectories are also shown next to the potential in Fig. 3 (a).

5.2.2 Protocol 2

We show Protocol 2 in Fig. 3 (b). Again, the system starts from a symmetric double-well potential, encoding information $H(p_0)$, and $E_b/kT = 13$. In this protocol, we first bring the system to a global equilibrium by equalizing the probability densities in two wells. We first stretch the right coordinate by the factor $\eta = 2$, as shown in Fig. 3 (b). We then lower the barrier and compress the right coordinate to its original scale. The rest of the protocol is the same as Protocol 1: we tilt, raise the barrier, and untilt.

Because of the stochastic nature of our system, we repeat such measurements for about 30 minutes for a fixed cycle time, after which we change the cycle time and repeat the measurements. For each cycle, we measure the stochastic work.

5.3 Work estimate

We estimate work from a single trajectory starting in a left w_{L}^i or right w_{R}^i well by discretizing Sekimoto's formula in Eq. 6. The mean work for a fixed cycle time is estimated via conditional work values. That is, we measure the average value of work W_{L} to erase conditioned on starting in the left well and similarly for the right well, W_{R}. For N_{L} and N_{R} individual measurements of w_{L}^i and w_{R}^i respectively, we estimate the mean via the average:

$$\begin{aligned} W_{\mathrm{L}} \approx \overline{W}_{\mathrm{L}} &= \frac{1}{N_{\mathrm{L}}} \sum_i w_{\mathrm{L}}^i \\ W_{\mathrm{R}} \approx \overline{W}_{\mathrm{R}} &= \frac{1}{N_{\mathrm{R}}} \sum_i w_{\mathrm{R}}^i \end{aligned} \tag{22}$$

The averages W_L and W_R are measured for both protocols and shown as a function of the inverse cycle time τ in Fig. 4. Error bars on work measurements in all cases represent the standard error of mean, calculated as $\sigma_W/\sqrt{N}$, with σ_W the standard deviation of the N individual measurements. The unconditional work at time τ is estimated from the law of total probability as $W_\tau = p_0 W_L + (1-p_0) W_R$.

The work in the *arbitrarily slow limit* W_∞, is obtained by extrapolating the average work values W_τ, which are measured at cycle times τ, to "infinitely" long cycle times. Operationally, we use the asymptotic form $W_\tau \sim W_\infty + a\tau^{-1}$ and fit a line against τ^{-1}.[68,69] The arbitrarily slow limit, obtained by extrapolating work measurements to infinite cycle times, is still faster than the barrier crossing time. Nevertheless, the barrier crossing time can be extremely long, because it grows so rapidly ($\propto e^{E_b}$) with barrier height E_b.[13]

Estimating the work in the arbitrarily slow limit for Protocol 1, we find $W_\infty^1/k_{\mathrm{B}}T = 0.67 \pm 0.05$. Similarly, for Protocol 2, we find $W_\infty^2/k_{\mathrm{B}}T = 0.58 \pm 0.07$. Protocol 1 requires more work than Protocol 2 to erase the same information $H(p_0)$.

5.4 Discussion

For Protocol 1, both conditional average work values are the same within the error bars. That is expected, because Protocol 1 applies the same transformations to the both, left and right, sides of the potential prior to lowering the barrier and mixing states. Protocol 2 treats left and right state separately, since it stretches only the right state, while the left state remains intact; therefore, we observe a difference in the mean work. After the two states are mixed into a single state, the remaining work is not conditioned on the initial state. We point out that a quantity of information $H(p_0)$ is erased at the moment when the barrier is lowered, and the two states are mixed. At that point, the system has only one degree of freedom, with information 0 according to Eq. 19. The rest of the protocol is designed to lock the system in this single degree of freedom and return the potential to its initial symmetric double-well form. Without these steps, the analysis in Eq. 21 should include a term giving the change in potential energy. The high barrier ensures that the system has only one degree of freedom over the time scales of interest.

5.5 Reversibility

Our measurement shows that Protocol 1 requires more work for erasing information $H(p_0)$ than Protocol 2. This is a consequence of the thermodynamic irreversibility of Protocol 1. But can we calculate the difference in work between two protocols? To calculate the required work in the arbitrarily slow limit, we can use recently developed tools of stochastic thermodynamics.[3,4] In particular, following the lead of Crooks,[70] we can compare the "forward" experimental trajectories with hypothetical "backwards" versions that result from reversing the protocol of potential manipulations. When Protocol 1, Fig. 3 (a), is played backwards, and a particle ends up in the left well with probability $\bar{p}_1 = 1/2$. That is not the case for Protocol 2. It ends up in the left well with probability $\bar{p}_2 = p_0 = 1/3$ when time reversed; therefore, Protocol 2 is thermodynamically reversible.

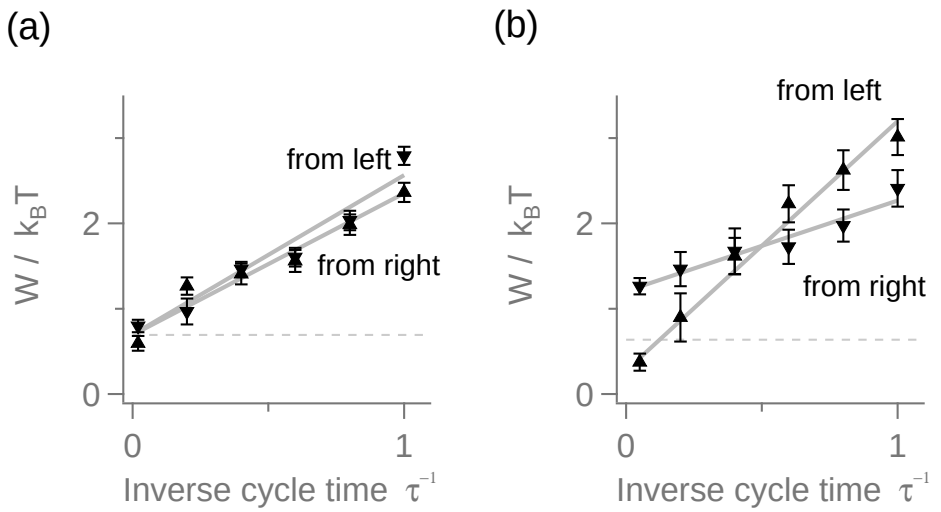

Figure 4. Protocols of duration τ for erasing a fraction of a bit, accompanied by sample trajectories. All end in the right well, which is achieved by strong tilt. (a) Protocol 1: less than one bit of memory is erased by directly mixing two states. This protocol is intrinsically dissipative, unless $p_0 = 0.5$. (b) Protocol 2: The potential is stretched to bring the two states to global equilibrium before mixing.

The average work in the arbitrarily slow limit can be estimated from the probabilities of each initial state p_0^* and the probability to end in each state in a backward process $\bar{p}^*$ as,

$$\frac{\langle W\rangle_\infty}{kT} = \Delta H + D_{\mathrm{KL}}(p_0^*||\bar{p}^*)\,, \tag{23}$$

where ΔH is the change in information or, in our case, the erased information $H(p_0)$. The Kullback-Leibler divergence $D_{\mathrm{KL}}(p_0^*||\bar{p}^*)$ is the "distance" between the probability distributions p_0^* and $\bar{p}^*$.[‡] Equation 23 applies to a system with several discrete states, and to a system where discrete states are indexed by i, and $D_{\mathrm{KL}}(p_0^*||\bar{p}^*) = \sum p_{0i} \ln(p_{0i}/\bar{p}_i)$. In our case, we have only two states that occur with the initial probabilities p_0 and $1-p_0$, and probabilities in backward process $\bar{p}^*$ and $1-\bar{p}^*$. Expanding the Kullback-Leibler divergence in Eq. 23 then gives

$$D_{\mathrm{KL}}(p_0^*||\bar{p}^*) = p_0 \ln\frac{p_0}{\bar{p}} + (1-p_0)\ln\frac{1-p_0}{1-\bar{p}}\,. \tag{24}$$

For Protocol 2, the expression in Eq. 24 gives 0, while for Protocol 1, it gives $\frac{5}{3}\ln(2) - \ln(3) \approx 0.06$; therefore, from Eq. 23, we expect Protocol 1 to require more work. This is also in accordance with our measurements in Sec 5.3, where the work for Protocol 1, $W_\infty^1/k_{\mathrm{B}}T = 0.67 \pm 0.05$, is greater than the work for Protocol 2 $W_\infty^2/k_{\mathrm{B}}T = 0.58 \pm 0.07$. Although the difference between the two values of $W/k_{\mathrm{B}}T \approx 0.09 \pm 0.078$ is consistent with the expected value of 0.06, the statistical errors cannot quite rule out the null hypothesis of identical means (Welch's t-test gives P=0.17).[§]

With planned technical improvements to our feedback trap, we will be able to improve our resolution by increasing the bandwidth of the feedback trap and acquiring more data. In Ref. 67, we present another approach using the time-reversal symmetry of the thermodynamically reversible protocol, a method that allows one to explore broad changes in information and for which the statistical errors are smaller. Nonetheless, here, we

[‡] Although not symmetric in its arguments, D_{KL} is positive for two different distributions and zero for two identical distributions.

[§] We calculate Welch's t statistic from the average work and standard error as $t = (W_\infty^1 - W_\infty^2)/\sqrt{\sigma_{W1}^2 + \sigma_{W2}^2} \approx 1.05$. The number of degrees of freedom is estimated as $\nu \approx (\sigma_{W1}^2 + \sigma_{W2}^2)^2 / \left[\sigma_{W1}^2/(1-N_1) + \sigma_{W2}^2/(1-N_2)\right] \approx 3.6$, where N_1 and N_2 are the degrees of freedom for the linear fit in Fig. 4.

have showed that our feedback trap has both the ability to implement very complex and versatile protocols and measure work to a high precision.

6. CONCLUSION

In this paper, we have used a feedback trap to erase a fraction of a bit of information and measure work for such an erasure. To achieve the minimal work for erasure, we designed a complex protocol that includes asymmetric stretching of a local coordinate, lowering the barrier, and tilting the potential. We also compare this complex protocol to a naive version, which cannot reach the ultimate thermodynamic limit. Our feedback trap is able to detect the work difference between two protocols to a high precision. In this case, the thermodynamical irreversibility of our naive protocol results in approximately 0.06 kT of extra work.

We have also reviewed some of the theoretical work in stochastic thermodynamics that is directly applicable to our experiment, and we have compared our feedback trap to other common tools and systems used for measurements in stochastic thermodynamics. We emphasize that a virtual potential imposed by a feedback trap is a perfect candidate for measurements in stochastic thermodynamics, because such measurements often require great flexibility for choosing and manipulating the form of the applied potential. This kind of flexibility is difficult, perhaps impossible, to achieve using physical potentials but is readily accomplished using feedback traps.

ACKNOWLEDGMENTS

We thank Raphaël Chétrite for helpful discussions. This work was supported by a Discovery Grant from NSERC (Canada).

REFERENCES

[1] Callen, H. B., [Thermodynamics and an Introduction to Thermostatistics], Wiley, 2nd ed. (1985).
[2] Ciliberto, S., "Experiments in stochastic thermodynamics: Short history and perspectives," Phys. Rev. X **7**, 021051 (2017).
[3] Sekimoto, K., [Stochastic Energetics], Springer (2010).
[4] Seifert, U., "Stochastic thermodynamics, fluctuation theorems and molecular machines," Rep. Prog. Phys. **75**(126001), 1–58 (2012).
[5] Maxwell, J. C., [Theory of Heat], Longmans, Green, and Co. (1871).
[6] Leff, H. S. and Rex, A. F., [Maxwell's Demon 2: Entropy, Classical and Quantum Information, Computing], IOP (2003).
[7] Wang, G. M., Sevick, E. M., Mittag, E., Searles, D. J., and Evans, D. J., "Experimental demonstration of violations of the second law of thermodynamics for small systems and short time scales," Phys. Rev. Lett. **89**, 050601 (2002).
[8] Liphardt, J., Dumont, S., Smith, S. B., Tinoco, I., and Bustamante, C., "Equilibrium information from nonequilibrium measurements in an experimental test of Jarzynski's equality," Science **296**(5574), 1832–1835 (2002).
[9] Toyabe, S., Sagawa, T., Ueda, M., Muneyuki, E., and Sano, M., "Experimental demonstration of information-to-energy conversion and validation of the generalized Jarzynski equality," Nature Phys. **6**, 988 (2010).
[10] Koski, J. V., Maisi, V. F., Pekola, J. P., and Averin, D. V., "Experimental realization of a Szilard engine with a single electron," PNAS **111**, 13786–13789 (2014).
[11] Bérut, A., Arakelyan, A., Petrosyan, A., Ciliberto, S., Dillenschneider, R., and Lutz, E., "Experimental verification of Landauer's principle linking information and thermodynamics," Nature **483**, 187–190 (2012).
[12] Jun, Y. and Bechhoefer, J., "Virtual potentials for feedback traps," Phys. Rev. E **86**, 061106 (2012).
[13] Gavrilov, M. and Bechhoefer, J., "Arbitrarily slow, non-quasistatic, isothermal transformations," EPL (Europhysics Letters) **114**(5), 50002 (2016).

[14] Cohen, A. E. and Moerner, W. E., "Method for trapping and manipulating nanoscale objects in solution," App. Phys. Lett. **86**, 093109 (2005).
[15] Cohen, A. E., "Control of nanoparticles with arbitrary two-dimensional force fields," Phys. Rev. Lett. **94**, 118102 (2005).
[16] Gavrilov, M., Jun, Y., and Bechhoefer, J., "Real-time calibration of a feedback trap," Rev. Sci. Instrum. **85**(9) (2014).
[17] Ashkin, A., Dziedzic, J. M., Bjorkholm, J. E., and Chu, S., "Observation of a single-beam gradient force optical trap for dielectric particles," Opt. Lett. **11**(5), 288–290 (1986).
[18] Berg-Sorensen, K. and Flyvbjerg, H., "Power spectrum analysis for optical tweezers," Rev. Sci. Instrum. **75**(3), 594–612 (2004).
[19] Berg-Sorensen, K., Peterman, E. J. G., Weber, T., Schmidt, C. F., and Flyvbjerg, H., "Power spectrum analysis for optical tweezers. II: Laser wavelength dependence of parasitic filtering, and how to achieve high bandwidth," Rev. Sci. Instrum. **77**(6) (2006).
[20] Collin, D., Ritort, F., Jarzynski, C., Smith, S. B., Tinoco, I., and Bustamante, C. T., "Verification of the Crooks fluctuation theorem and recovery of RNA folding free energies," Nature (2005).
[21] Carlson, C. A., Sweeney, N. L., Nasse, M. J., and Woehl, J. C., "The corral trap: fabrication and software development," Proc. SPIE **7571**, 757108–757108–6 (2010).
[22] Roldán, É., Martínez, I. A., Parrondo, J. M. R., and Petrov, D., "Universal features in the energetics of symmetry breaking," Nature Phys. **10**, 457–461 (2014).
[23] Martínez, I. A., Roldán, E., Dinis, L., Petrov, D., and Rica, R. A., "Adiabatic processes realized with a trapped Brownian particle," Phys. Rev. Lett. **114**, 120601 (2015).
[24] Martínez, I. A., Roldán, É., Dinis, L., Petrov, D., Parrondo, J. M. R., and Rica, R. A., "Brownian Carnot engine," Nature Phys. **12**(1), 67–70 (2016).
[25] Blickle, V. and Bechinger, C., "Realization of a micrometre-sized stochastic heat engine," Nature Phys. **8**(2), 143–146 (2012).
[26] Braun, M., Bregulla, A. P., Gunther, K., Mertig, M., and Cichos, F., "Single molecules trapped by dynamic inhomogeneous temperature fields," Nano Lett. **15**(8), 5499–5505 (2015).
[27] Shenoy, A., Tanyeri, M., and Schroeder, C. M., "Characterizing the performance of the hydrodynamic trap using a control-based approach," Microfluid Nanofluidics **18**(5), 1055–1066 (2015).
[28] Lutz, B. R., Chen, J., and Schwartz, D. T., "Hydrodynamic tweezers: Noncontact trapping of single cells using steady streaming microeddies," Anal. Chem. **78**(15), 5429–5435 (2006).
[29] Schroeder, C. M., Shaqfeh, E. S. G., and Chu, S., "Effect of hydrodynamic interactions on DNA dynamics in extensional flow: Simulation and single molecule experiment," Macromolecules **37**(24), 9242–9256 (2004).
[30] Armani, M. D., Chaudhary, S. V., Probst, R., and Shapiro, B., "Using feedback control of microflows to independently steer multiple particles," J. Microelectromech Syst. **15**, 945–956 (2006).
[31] Tanyeri, M., Johnson-Chavarria, E. M., and Schroeder, C. M., "Hydrodynamic trap for single particles and cells," Applied Phys. Lett. **96**(22) (2010).
[32] Tanyeri, M. and Schroeder, C. M., "Manipulation and confinement of single particles using fluid flow," Nano Lett. **13**(6), 2357–2364 (2013).
[33] Sekimoto, K., "Kinetic characterization of heat bath and the energetics of thermal ratchet models," J. Phys. Soc. Jap. **66**, 1234–1237 (1997).
[34] Blickle, V., Speck, T., Helden, L., Seifert, U., and Bechinger, C., "Thermodynamics of a colloidal particle in a time-dependent nonharmonic potential," Phys. Rev. Lett. **96**, 070603 (2006).
[35] Klages, R., Just, W., and Jarzynski, C., eds., [Nonequilibrium Statistical Physics of Small Systems: Fluctuation Relations and Beyond], Wiley-VCH (2013).
[36] Gavrilov, M. and Bechhoefer, J., "Feedback traps for virtual potentials," Phil. Trans. R. Soc. A **375**, 20160217 (2017).
[37] Jarzynski, C., "Nonequilibrium equality for free energy differences," Phys. Rev. Lett. **78**, 2690–2693 (1997).
[38] Douarche, F., Ciliberto, S., Petrosyan, A., and Rabbiosi, I., "An experimental test of the Jarzynski equality in a mechanical experiment," EPL (Europhysics Letters) **70**(5), 593 (2005).

[39] Harris, N. C., Song, Y., and Kiang, C.-H., "Experimental free energy surface reconstruction from single-molecule force spectroscopy using Jarzynski's equality," Phys. Rev. Lett. **99**, 068101 (2007).
[40] Bérut, A., Petrosyan, A., and Ciliberto, S., "Detailed Jarzynski equality applied to a logically irreversible procedure," EPL **103**, 60002 (2013).
[41] Jun, Y., Gavrilov, M., and Bechhoefer, J., "High-precision test of Landauer's principle in a feedback trap," Phys. Rev. Lett. **113**, 190601 (2014).
[42] Luccioli, S., Imparato, A., and Torcini, A., "Free-energy landscape of mechanically unfolded model proteins: Extended Jarzinsky versus inherent structure reconstruction," Phys. Rev. E **78**, 031907 (2008).
[43] Gupta, A. N., Vincent, A., Neupane, K., Yu, H., Wang, F., and Woodside, M. T., "Experimental validation of free-energy-landscape reconstruction from non-equilibrium single-molecule force spectroscopy measurements," Nature Phys. **7**(8), 631–634 (2011).
[44] von Neumann, J., [Theory of Self-Reproducing Automata], University of Illinois Press, Urbana (1966).
[45] Landauer, R., "Irreversibility and heat generation in the computing process," IBM J. Res. Develop. **5**, 183–191 (1961).
[46] Szilard, L., "On the decrease of entropy in a thermodynamic system by the intervention of intelligent beings," Z. Physik **53**, 840–856 (1929).
[47] image, D., "https://commons.wikimedia.org/wiki/File:Daemon-phk.png."
[48] Still, S., "Thermodynamic cost and benefit of data representations," arXiv preprint arXiv:1705.00612 (2017).
[49] Brillouin, L., "Maxwell's demon cannot operate: Information and entropy. I," J. Appl. Phys. **22**(3), 334–337 (1951).
[50] Bennett, C. H., "The thermodynamics of computation: a review," Int. J. Theor. Phys. **21**, 905–940 (1982).
[51] Penrose, O., [Foundations of Statistical Mechanics: A Deductive Treatment], Pergamon (1970).
[52] Cohen, A. E. and Moerner, W. E., "Suppressing Brownian motion of individual biomolecules in solution," PNAS **103**, 4362–4365 (2006).
[53] Wang, Q. and Moerner, W. E., "Single-molecule motions enable direct visualization of biomolecular interactions in solution," Nat. Methods **11**(5), 556–558 (2014).
[54] Cohen, A. E. and Moerner, W. E., "Principal-components analysis of shape fluctuations of single DNA molecules," PNAS **104**, 12622–12627 (2007).
[55] Goldsmith, R. H. and Moerner, W. E., "Watching conformational- and photodynamics of single fluorescent proteins in solution," Nature Chem. **2**, 179–186 (2010).
[56] Fields, A. P. and Cohen, A. E., "Electrokinetic trapping at the one nanometer limit," PNAS **108**, 8937–8942 (2011).
[57] Germann, J. A. and Davis, L. M., "Three-dimensional tracking of a single fluorescent nanoparticle using four-focus excitation in a confocal microscope," Opt. Express **22**, 5641–5650 (2014).
[58] Kayci, M., Chang, H.-C., and Radenovic, A., "Electron spin resonance of nitrogen-vacancy defects embedded in single nanodiamonds in an ABEL trap," Nano Lett. **14**, 5335–5341 (2014).
[59] Gavrilov, M., Jun, Y., and Bechhoefer, J., "Particle dynamics in a virtual harmonic potential," Proc. SPIE **8810** (2013).
[60] Lee, D. Y., Kwon, C., and Pak, H. K., "Nonequilibrium fluctuations for a single-particle analog of gas in a soft wall," Phys. Rev. Lett. **114**, 060603 (2015).
[61] Gavrilov, M., Koloczek, J., and Bechhoefer, J., "Feedback trap with scattering-based illumination," in [Novel Techniques in Microscopy], JT3A. 4, Opt. Soc. Am. (2015).
[62] Gavrilov, M. and Bechhoefer, J., "Erasure without work in an asymmetric, double-well potential," Phys. Rev. Lett. **117**, 200601 (2016).
[63] Proesmans, K., Dreher, Y., Gavrilov, M. c. v., Bechhoefer, J., and Van den Broeck, C., "Brownian duet: A novel tale of thermodynamic efficiency," Phys. Rev. X **6**, 041010 (2016).
[64] Berglund, A. J., McMahon, M. D., McClelland, J. J., and Liddle, J. A., "Fast, bias-free algorithm for tracking single particles with variable size and shape," Opt. Express **16**, 14064–14075 (2008).
[65] Åström, K. J. and Wittenmark, B., [Adaptive Control], Dover, 2nd ed. (2008).
[66] Bechhoefer, J., "Feedback for physicists: A tutorial essay on control," Rev. Mod. Phys. **77**, 783–836 (2005).

[67] Gavrilov, M., Chétrite, R., and Bechhoefer, J., "Direct measurement of nonequilibrium system entropy is consistent with gibbs-shannon form," arXiv preprint arXiv:1703.07601 (2017).
[68] Sekimoto, K. and Sasa, S., "Complementarity relation for irreversible process derived from stochastic energetics," J. Phys. Soc. Jap. **66**(11), 3326–3328 (1997).
[69] Aurell, E., Gawędzki, K., Mejía-Monasterio, C., Mohayaee, R., and Muratore-Ginanneschi, P., "Refined second law of thermodynamics for fast random processes," J. Stat. Phys. **147**, 487–505 (2012).
[70] Crooks, G. E., "Entropy production fluctuation theorem and the nonequilibrium work relation for free energy differences," Phy. Rev. E **60**, 2721–2726 (1999).